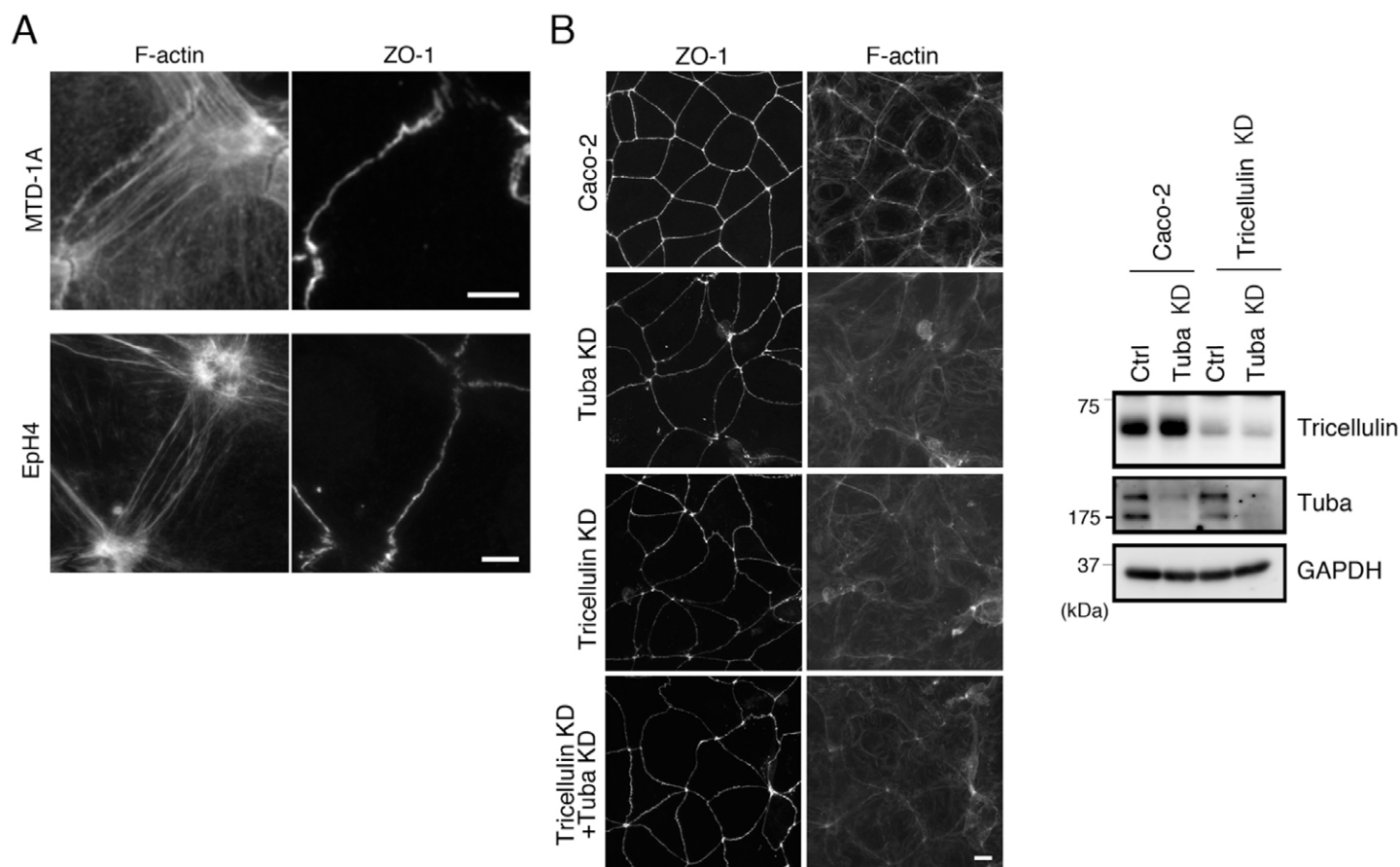
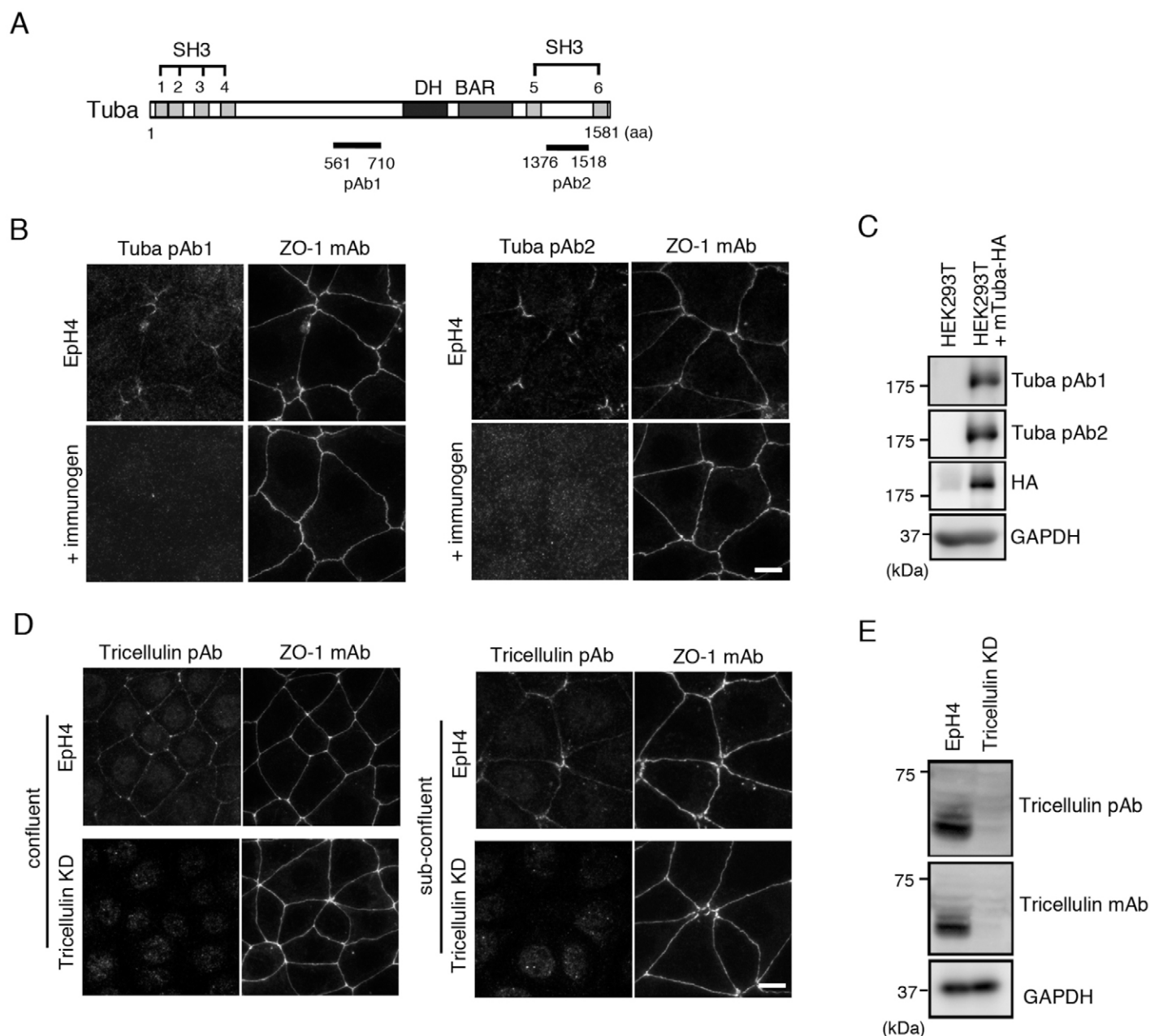


**Fig. S1.** (A) Original images for quantification of the number of rosette-like structures in MTD-1A cells and two clones of tricellulin knockdown cells (Tricellulin KD1 and Tricellulin KD2) presented in Figure 1D. The numbers of regions where more than five cell vertices were crowded together within a circle of 5-mm diameter (red circles) in immunofluorescence staining images with an anti-ZO-1 antibody were counted. Three independent measurements were performed for each cell type. Bar, 20 mm. (B) TUNEL assays of tricellulin knockdown MTD-1A cells during rosette-like structure formation. MTD-1A cells and Tricellulin KD1 cells at 24 and 48 h after plating were processed for TUNEL assays using a Click-it TUNEL Imaging Assay (Molecular Probes). As a positive control for apoptosis, MTD-1A cells at 24 h after plating were treated with 5 mM staurosporine for 3 h, cultured with normal medium for a further 21 h, and then processed for TUNEL assays. Each panel shows the merged image of apoptotic nuclei (green) and immunostaining for ZO-1 (red). At each time point for Tricellulin KD1 cells, apoptotic nuclei are hardly detected, suggesting that the rosette-like structures of Tricellulin KD1 cells observed at 48 h after plating are not caused by cell extrusion from the cellular sheet via apoptosis. Bar, 10 mm.



**Fig. S2.** (A) High-magnification images of PEC-PEC F-actin fibers. PEC-PEC fibers of F-actin in MTD-1A cells and Eph4 cells were visualized by fluorescent phalloidin staining. The cells were counterstained with an anti-ZO-1 antibody to delineate cell-cell junctions. The experimental conditions are the same as those for Figure 2A, B. Bars, 5 mm. (B) Immunofluorescence staining of Caco-2 cells, Tuba siRNA-treated Caco-2 cells (Tuba KD), tricellulin siRNA-treated Caco-2 cells (Tricellulin KD), and Caco-2 cells treated with both tricellulin siRNA and Tuba siRNA (Tricellulin KD+Tuba KD) at 48 h after plating using an anti-ZO-1 antibody with fluorescently labeled phalloidin. Bar, 10 mm. The immunoblots indicate the expressions of tricellulin and Tuba in Caco-2 cells, Tuba siRNA-treated Caco-2 cells, tricellulin siRNA-treated Caco-2 cells, and Caco-2 cells treated with both tricellulin siRNA and Tuba siRNA from the left.



**Fig. S3.** Characterization of rabbit anti-mouse Tuba polyclonal antibodies and a rat anti-tricellulin polyclonal antibody. (A) Schematic representation of mouse Tuba, which contains six SH3 domains, one DH domain and one BAR domain. Rabbit anti-Tuba polyclonal antibodies 1 (pAb1) and 2 (pAb2) were raised against GST fusion proteins with aa 561–710 and aa 1376–1518 of mouse Tuba, respectively. (B) Immunofluorescence staining of EpH4 cells in a subconfluent condition with anti-Tuba antibodies pAb1 and pAb2 in the absence and presence of their corresponding immunogens. Both antibodies show identical staining patterns at cell corner regions, and this staining disappears after addition of their immunogens, indicating the specificity of these antibodies in immunofluorescence staining. The cells were counterstained with a mouse anti-ZO-1 monoclonal antibody to delineate cell–cell contacts. Bar, 10  $\mu$ m. (C) Western blotting of HEK293 cells transfected with control vector or an expression vector for mouse Tuba-HA using two anti-Tuba antibodies (pAb1 and pAb2), an anti-HA antibody and an anti-GAPDH antibody. (D) Double immunofluorescence staining of EpH4 cells and tricellulin knockdown EpH4 cells (Tricellulin KD) in confluent and subconfluent conditions with a rat anti-tricellulin polyclonal antibody (Tricellulin pAb) and a mouse anti-ZO-1 monoclonal antibody. The characteristic staining pattern of tricellulin at cell corner regions of subconfluent EpH4 cells is not detected in Tricellulin KD cells, indicating that this staining is tricellulin-specific. Bars, 10  $\mu$ m. (E) Western blotting of EpH4 and Tricellulin KD cells with antibodies for tricellulin and GAPDH.



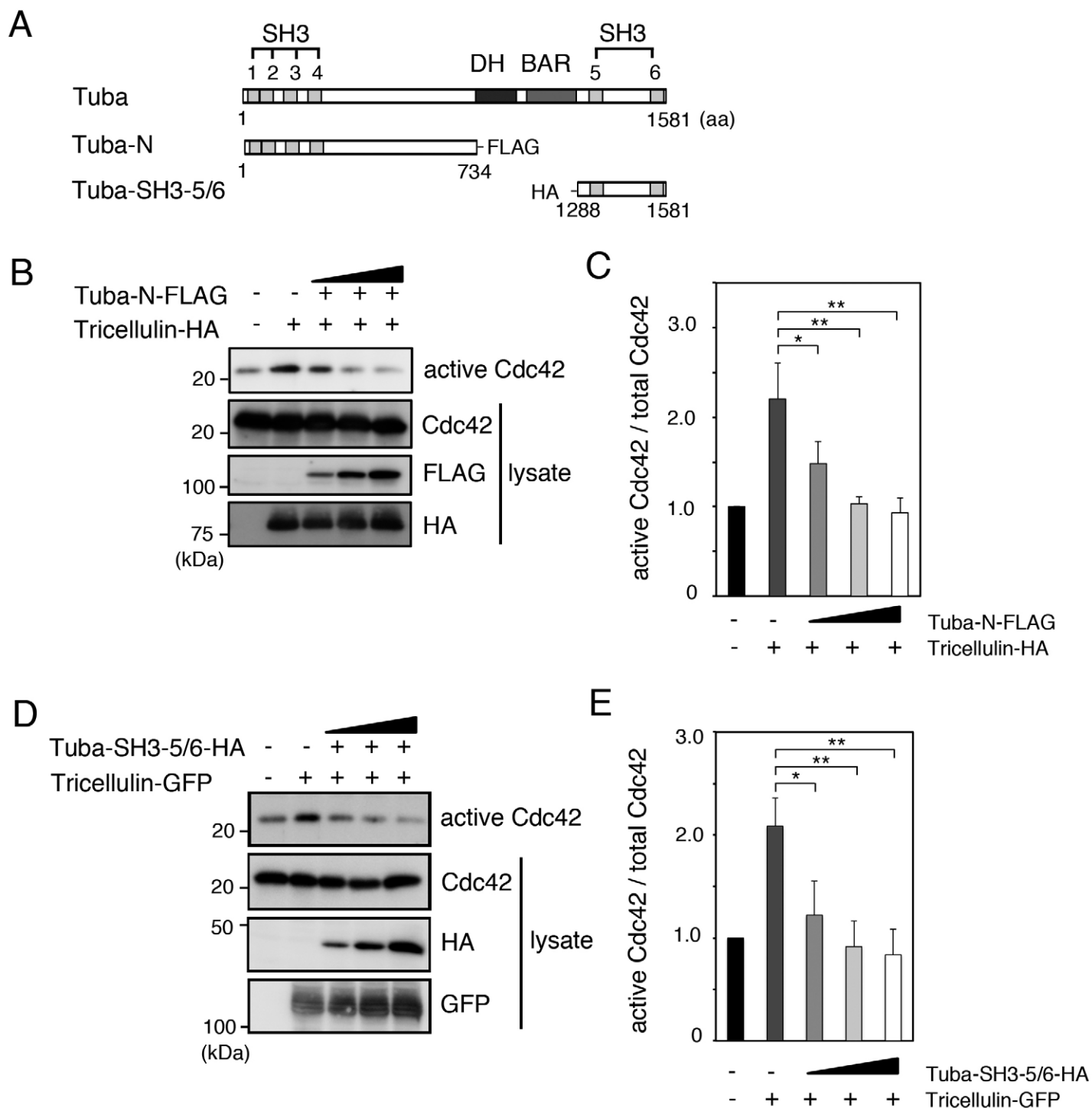


**Fig. S4.** Inhibition of tricellulin-mediated Cdc42 activation by the addition of Tuba fragments. (A) Schematic diagrams of full-length Tuba and its deletion constructs. Tuba-SH3-5/6 contains only the fifth and sixth SH3 domains tagged with HA. (B) Inhibition of tricellulin-induced Cdc42 activation by expression of the N-terminal half of Tuba. HEK293 cells were transfected with expression vectors for HA-tagged tricellulin and FLAG-tagged Tuba-N, which were added in a dose-dependent manner. The active form of Cdc42 was detected as shown in Fig. 7B. Whole cell lysates (lysate) were immunoblotted with antibodies for HA, FLAG and Cdc42. (C) Quantitative analysis of active Cdc42 in (B) calculated according to the method in Fig. 7C. (D) Inhibition of tricellulin-induced Cdc42 activation by expression of the C-terminal fragment of Tuba containing the C-terminal two SH3 domains. HEK293 cells were transfected with expression vectors for GFP-tagged tricellulin and HA-tagged Tuba-SH3-5/6, which were added in a dose-dependent manner. The active form of Cdc42 was detected as shown in Fig. 7B. Whole cell lysates (lysate) were immunoblotted with antibodies for HA, GFP and Cdc42. (E) Quantitative analysis of active Cdc42 in (D) calculated according to the method in Fig. 7C.